

See discussions, stats, and author profiles for this publication at: <https://www.researchgate.net/publication/40448226>

Micronozzle Array Enhanced Sandwich Electroporation of Embryonic Stem Cells

ARTICLE *in* ANALYTICAL CHEMISTRY · DECEMBER 2009

Impact Factor: 5.64 · DOI: 10.1021/ac902041h · Source: PubMed

CITATIONS

25

READS

11

6 AUTHORS, INCLUDING:



Xin Hu

Schlumberger Limited

33 PUBLICATIONS 265 CITATIONS

SEE PROFILE



Hae-Woon Choi

Keimyung University

48 PUBLICATIONS 414 CITATIONS

SEE PROFILE



D. F. Farson

The Ohio State University

81 PUBLICATIONS 1,142 CITATIONS

SEE PROFILE

Micronozzle Array Enhanced Sandwich Electroporation of Embryonic Stem Cells

Zhengzheng Fei,^{†,‡} Xin Hu,[†] Hae-woon Choi,^{†,§,⊥} Shengnian Wang,^{†,||} Dave Farson,^{†,§} and L. James Lee^{*,†,‡}

Nanoscale Science and Engineering Center for Affordable Nanoengineering of Polymeric Biomedical Devices, Department of Chemical and Biomolecular Engineering, and Department of Industry, Welding and System Engineering, The Ohio State University, Columbus, OH

Electroporation is one of the most popular nonviral gene transfer methods for embryonic stem cell transfection. Bulk electroporation techniques, however, require a high electrical field and provide a nonuniform electrical field distribution among randomly distributed cells, leading to limited transfection efficiency and cell viability, especially for a low number of cells. We present here a membrane sandwich electroporation system using a well-defined micronozzle array. This device is capable of transfecting hundred to millions of cells with good performance. The ability to treat a small number of cells (i.e., a hundred) offers great potential to work with hard-to-harvest patient cells for pharmaceutical kinetic studies. Numerical simulation of the initial transmembrane potential distribution and propidium iodide (PI) dye diffusion experiments demonstrated the advantage of highly focused and localized electric field strength provided by the micronozzle array over conventional bulk electroporation.

Over the past decade, the use of genetically modified embryonic stem (ES) cells has become an attractive tool for fundamental studies as well as clinical applications.^{1–3} For example, recent studies in cell culture systems indicated that it is possible to introduce the gene *Nurr1* into ES cells to regulate the formation of dopamine-producing nerve cells for the treatment of Parkinson's disease.^{4,5}

Viral transduction of ES cells is very efficient, but safety issues, such as immune and inflammatory responses, have hampered

their clinical use in humans.^{6,7} Bulk electroporation is one of the most popular nonviral gene transfer methods for ES cell transfection.⁸ However, a large number of cells are often required (10^6 – 10^7 for a cuvette and 5×10^4 – 2×10^5 for a well of a 96 well plate⁹) to obtain acceptable gene transfection and cell viability. This is because most of the cell surface is affected by the applied high electric field and the shading effect¹⁰ often prevents uniform transfection due to the randomly suspended cells and genes in the bulk electroporation process. Although nucleofection, the best known commercial electroporation technique, has demonstrated very good transfection efficiency, it relies on an expensive electroporation buffer that varies from cell to cell. Neither the recipes of the cell-dependent electroporation buffer nor the electrical parameters are disclosed by the manufacturer.¹¹ There are also concerns that the unknown additives in the electroporation buffer may affect the behavior of transfected cells. We have recently developed a membrane sandwich electroporation (MSE) technique¹² using track-etched membranes. Because of localized electroporation and better gene confinement near the cell surface, our MSE method is capable of achieving good transfection efficiency and high cell viability using a small number of cells, as low as several hundreds.

However, the previous design could not provide a uniform electric field distribution to each cell because of randomly distributed pores on the track-etched membrane. Consequently, the gene transfection efficiency was limited. To address this limitation, we form a well-defined micropore array on nanoporous polyethylene terephthalate (PET) track-etched membranes using femtosecond pulsed laser ablation. By adjusting the laser output power and laser beam focus point, we are able to produce both converging micronozzle and straight microchannel arrays on the membrane. This new design is tested by plasmid pmaxGFP and plasmid gWiz SEAP transfection of mouse ES cells. The observed transfection results are explained by numerical calculations of the transmembrane potential (potential difference across the cell

* Corresponding author. Phone: 614-292-2408. Fax: 614-292-8685. E-mail: lee.31@osu.edu.

[†] Nanoscale Science and Engineering Center for Affordable Nanoengineering of Polymeric Biomedical Devices.

[‡] Department of Chemical and Biomolecular Engineering.

[§] Department of Industry, Welding and System Engineering.

[⊥] Current address: Department of Mechanical & Automotive Engineering, Keimyung University, Daegu, South Korea.

^{||} Current address: Institute for Micromanufacturing, Louisiana Tech University, Ruston, LA.

(1) Ben-Nuna, I. F.; Benvenisty, N. *Mol. Cell. Endocrinol.* **2006**, *252*, 154–159.

(2) O'Connor, T. P.; Crystal, R. G. *Nat. Rev. Genet.* **2006**, *7*, 261–276.

(3) Strulovici, Y.; Leopold, P. L.; O'Connor, T. P.; et al. *Mol. Ther.* **2007**, *15*, 850–866.

(4) Kim, J. H.; Auerbach, J. M.; Rodriguez-Gomez, J. A.; et al. *Nature* **2002**, *418*, 50–56.

(5) Lindvall, O.; Kokaia, Z. *Nature* **2006**, *441*, 1094–1096.

(6) Thomas, C. E.; Ehrhardt, A.; Kay, M. A. *Nat. Rev. Genet.* **2003**, *4*, 346–358.

(7) Niidome, T.; Huang, L. *Gene Ther.* **2002**, *9*, 1647–1652.

(8) Tompers, D. M.; Labosky, P. A. *Stem Cells* **2004**, *22*, 243–249.

(9) <http://www.amaxa.com/research-areas/stem-cell-research/>.

(10) Reberšek, M.; Faurie, C.; Kandušer, M.; Čorović, S.; Teissié, J.; Rols, M.-P.; Miklavčič, D. *BioMed. Eng. OnLine* **2007**, *6*, 25.

(11) <http://www.biocompare.com/Articles/ProductReview/933/Nucleofector-96-well-Shuttle-From-Amata-Biosystems.html>.

(12) Fei, Z.; Wang, S.; Xie, Y.; et al. *Anal. Chem.* **2007**, *79*, 5719–572.

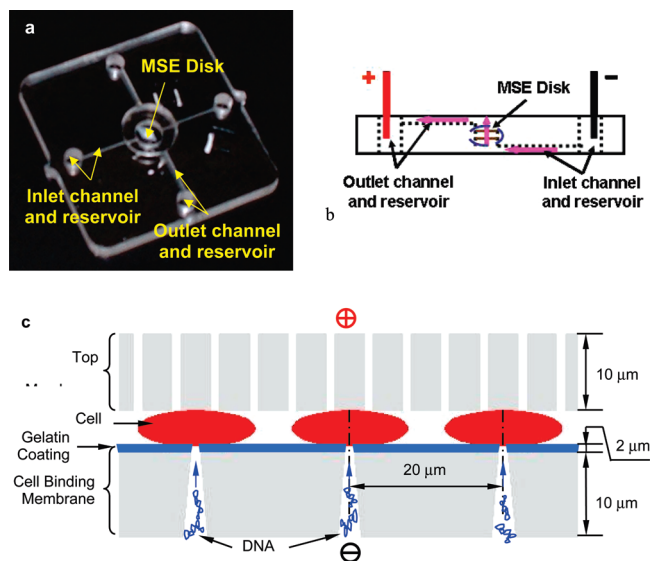


Figure 1. (a) MSE device. (b) Schematic of DNA migration path in the MSE device (pink arrow). (c) Schematic of MSE disk setup.

membrane) distribution on the cell surface.

MATERIALS AND METHODS

Cell Line and Plasmids. Mouse ES cells (CCE strain) were purchased from StemCell Technologies Inc. (Vancouver, BC, Canada). Cell culture media and reagents were purchased from invitrogen (Carlsbad, CA) unless otherwise specified. Plasmid pmaxGFP (3.5 kbp) were purchased from Lonza Group Ltd. (Switzerland), and gWiz SEAP (6.6 kbp) were purchased from Aldevron (Fargo, ND).

Embryonic Stem Cell Culture. Mouse ES cells were maintained in an undifferentiated state on 0.1% (w/v) gelatin coated dishes in high glucose Dulbecco's Modified Eagle's Medium (DMEM with 4500 mg of D-glucose/L, StemCell Technologies, Catalog No. 36250) supplemented with 15% ES-Cult fetal bovine serum (FBS, StemCell Technologies, Catalog No. 06952), 2 mM L-glutamine (Catalog No. 25030), 1 mM MEM sodium pyruvate (Catalog No. 11360), 1000 U/mL recombinant mouse leukemia inhibitory factor (rm LIF, Millipore, Catalog No. LIF2010), 100 U/mL penicillin G + 10 μ g/mL streptomycin (Catalog No. 15140), 0.1 mM MEM nonessential amino acids (NEAA, Catalog No. 11140), and 150 μ M monothioglycerol (MTG, Sigma-Aldrich, Catalog No. M6145).

Mouse ES cells were cultured at 37 °C with 5% CO₂, and passaged every 3 days by trypsinization. Mouse ES cells were typically used when reaching 50–70% confluency.

Fabrication of MSE Device. The MSE device consists of a pair of cross channels connected by a center hole as shown in Figure 1a. One channel is present on the top of the device, and the other is on the bottom. Both channels are 500 μ m in width and depth. The channel on the top of the device intersects with a 1 cm diameter reservoir located at the center of the device where membranes can be fixed to the device.

The MSE device was fabricated in a poly(methyl methacrylate) (PMMA) substrate using a high precision computer numerically controlled machine (AeroTech Inc., Pittsburgh, PA). A 45 μ m thick PMMA film was bonded to the back side of the device using a thermal film laminator (Catena 35, GBC, Addison, IL), enclosing

the bottom channel but allowing top access via reservoirs at the ends.

Femtosecond Laser (FS) Drilling of Gelatin-Coated PET Membrane. A Ti:Al₂O₃ based regenerative amplifier laser (CPA2161, Clark-MXR) was used as a femtosecond laser energy source. It has a central wavelength of 775 nm, pulse duration of 150 fs, and pulse repetition frequency of 3 kHz. The maximum output power of the system is 2.6 W, and it was attenuated to the milliwatt scale by thin-film polarizing beam splitters (PBS) and a $\lambda/2$ wave plate. A 50 \times infinity corrected microscope objective lens with numerical aperture (NA) of 0.42 (50 \times M Plan Apo NIR, Mitutoyo) was used for fine focusing. Attenuated laser power was measured by a power meter (PM100, Thorlab) placed right under the laser focusing lens.^{13,14}

PET membranes with 0.4 μ m pores were coated with 0.1% (w/w) gelatin at room temperature for 30 min, yielding a thin layer with thickness of 2 to 3 μ m. Different output laser beam powers up to 6 mW were tested to determine the desirable power range for a minimal thermal effect on the surrounding gelatin-coated surface. Multiple laser beam powers were used to drill the micropore array on a gelatin-treated PET membrane. When the laser beam power pattern is varied, the shape and the size of micropores could be controlled. Pore characterization was carried out using a scanning electron microscope (SEM, Hitachi S-4300 Field Emission). To perform SEM, a thin (50 nm) gold layer was sputter-coated on the samples using an Emitech k550x sputter coater.

Electroporation Procedure. Nucleofection by Amaxa Biosystem. Mouse ES cells were pelleted via centrifugation and washed twice with Dulbecco's phosphate-buffered saline (D-PBS, pH 7.4, Invitrogen, Catalog No. 14190). One million (1×10^6) cells were then resuspended in transfection solution from a Mouse ES Cell Nucleofector kit (Amaxa, Catalog No. VPH-1001) with 200 ng/ μ L plasmids and transferred to the 2 mm gap nucleofection cuvette. Mouse ES cells were nucleoporated at Program A-13, A-23, A-24, and A-30 according to the manufacturer's suggestion, and A-23 was selected in this study (Figure S1 in the Supporting Information).

Bulk Electroporation by Bio-Rad Gene Pulser X-Cell System. Mouse ES cells were pelleted via centrifugation and washed twice with D-PBS. The pellet was resuspended in high glucose DMEM and then transferred to the 1 mm or 2 mm electroporation cuvette (Bio-Rad). Two different cell concentrations were tested as shown in Table 1. The electroporation parameters were optimized (Figure S2 in the Supporting Information), and the best electroporation condition is shown in Table 1.

Micropore Array Enhanced MSE. A gelatin-coated PET membrane with micropore arrays drilled by a femtosecond pulsed laser was used as the cell binding membrane. Briefly, the cell binding membrane was mounted at the center reservoir of the fluidic device. A drop of suspended cells was loaded onto the support membrane, and a vacuum of 34 ± 3 kPa was used to trap the cells on the support membrane. Another PET track-etched membrane with an average pore size of 1 μ m was placed over the immobilized cells. The cells were sandwiched between two membranes sealed

(13) Farsona, D. F.; Choi, H. W.; Lu, C.; et al. *J. Laser Appl.* **2006**, *18*, 210–215.

(14) Farsona, D. F.; Choi, H. W.; Zimmerman, B. J. *Micromech. Microeng.* **2008**, *18*, 035020/1–9.

Table 1. Comparison of Nucleofection, Conventional Bulk Electroporation by Bio-Rad Gene Pulser X-Cell System, and Membrane Sandwich Electroporation (MSE)

method	nucleofection	bulk electroporation		MSE
pulse type	unknown	exponential decay		
pulse number	unknown	1		1
field strength (V/cm)	unknown	500		150
capacitance (μF)	unknown	500		500
DNA concentration ($\mu\text{g/mL}$)	200	200	50	5
initial cell number	1×10^6	1×10^6	1×10^5	1×10^4
cuvette	2 mm	2 mm	1 mm	N/A
total buffer volume (μL)	100	100	100	200

together (Figure 1b). The bottom channel and inlet reservoirs were loaded with high glucose DMEM with 5 ng/ μL DNA, and the top channel and outlet reservoirs were then loaded with high glucose DMEM. A low DC voltage of 10 V was applied to the system for 5 s; DNA molecules were migrated from the cathode to the MSE disk (Figure 1c) and concentrated in the micropores of the cell binding membrane. Finally, the cells were pulsed with a single exponential decay pulse at 150 V/cm and 500 μF (Table. 1), and the MSE disk was transferred to a 48 well plate with 250 μL of culture media in each well.

Assay for Transfection Efficiency and Cell Viability. The transfection efficiency of pmaxGFP in mouse ES cells was qualified by the percentage of the cells with green fluorescence among the cells observed by phase contrast in the same visual area.

The transfection efficiency of gWiz SEAP was expressed as the total SEAP activity per ten thousand initial input cells. Samples of culture media were collected 48 h after electroporation and determined by a colorimetric assay based on the hydrolysis of *p*-nitrophenyl phosphate (pNPP). The pNPP substrate solution was fresh prepared using SIGMAFAST pNPP tablets (Sigma-Aldrich, Catalog No. N1891, St. Louis, MO). Culture media (100 μL) and 25 μL of pNPP substrate solution were added into each well of a 96 well plate. The plate was incubated in the dark for approximately 15 min at room temperature and read at the wavelength of 405 nm on a multiwell plate reader (GENios Pro, Tecan, Durham, NC).

A CellTiter 96 nonradioactive cell proliferation assay (MTS) was used to measure the cell viability at 24 h postelectroporation. MTS reagent was diluted in culture media at 1:10, and the work solution was then added to the culture wells. The absorbance at 570 nm was recorded after 2 h of incubation at 37 $^{\circ}\text{C}$ with 5% CO_2 .

RESULTS AND DISCUSSION

Femtosecond (FS) Laser Drilling of Gelatin-Treated PET Membrane. FS laser is an excellent tool for direct micropatterning of biomaterials. Because of the ultrashort contact between the laser beam and materials, there is very low heat transfer to surrounding materials. Gelatin has been widely used as a feeder-free substrate for maintaining mouse ES cells in an undifferentiated status. Multiple wells were produced by scanning the focused femtosecond pulsed laser beams under various powers over the gelatin-coated PET surface. After sterilization, mouse ES cells were seeded at a desired density to determine the heat effect on the bioactivity of the surrounding gelatin-coated surface. Figure 2a shows the morphology and distribution of mouse ES cells after a 2 day culture. Mouse ES cells grew very well around the wells at

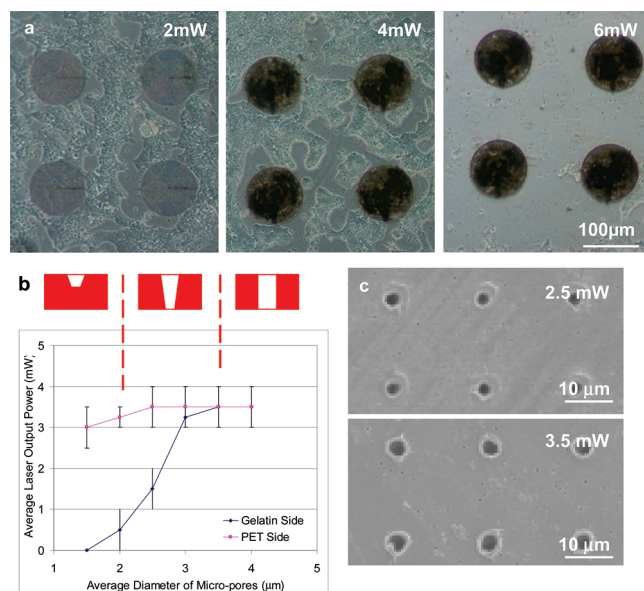


Figure 2. (a) Heat effect of various laser beam power on the surrounding gelatin-coated PET surface; (b) shape and size of the micropores produced under various laser beam power up to 4 mW; (c) SEM images of micropores on the gelatin coating side produced at the average laser beam power of 2.5 (upper) and 3.5 mW (lower).

both 2 and 4 mW, while nearly no mouse ES cells were observed on the surrounding surface of the wells milled at 6 mW. This implies that an average output laser beam power of up to 4 mW can provide proper irradiance incident to fabricate the gelatin-coated PET surface without denaturing the gelatin coating.

A range of laser beam power from 1 to 4 mW was then used to drill a periodic array of micropores in a gelatin-coated PET membrane. SEM images were taken to determine the dimension and surface roughness of micropores. The relationship between pore dimension and laser beam power is plotted in Figure 2b. Smooth and well-defined micropores with minimal gelatin denaturing was obtained by FS laser drilling at relatively low pulse energies in our work, but a pulse energy below 2 mW was not high enough to penetrate the gelatin-coated PET membrane. Two different micropore shapes were generated: a converging nozzle at the laser output power between 2 and 3.5 mW and a straight channel at the output laser power higher than 3.5 mW. Figure 2c shows SEM images of micropores on the gelatin coating side produced under an average output power of 2.5 and 3.5 mW, respectively, on a gelatin-coated PET membrane. Under 2.5 mW, the average pore size was 3.5 μm on the PET membrane side

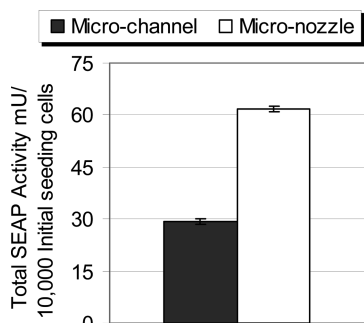


Figure 3. Effect of different pore shapes, microchannel (■) and micronozzle (□), on mouse ES cell transfection by MSE. The bars indicate total activity of SEAP expression 24 h after MSE under the optimized electrical field. (See Figure S3 in the Supporting Information.)

and 1.5 μm on the gelatin coating side, while the average pore size for both sides was 3.5 μm under 3.5 mW.

Effect of Micropore Shape on Transfection Efficiency. To determine the effect of micropore shape on the MSE performance, mouse ES cells were transfected by the MSE method with the converging micronozzle array and the straight microchannel array. The converging micronozzles were obtained at the output laser power of 2.5 mW, and the straight microchannels were fabricated under 3.5 mW. Plasmids gWiz SEAP were used as reporter genes, and SEAP transfection of mouse embryonic stem cells on the 100×100 array was evaluated 24 h after electroporation. As shown in Figure 3, SEAP expression using the micronozzles almost doubled over that with microchannels, mainly because the electric field is more concentrated at the small-end of the micronozzle, resulting in better localized electroporation. This will be further explained by numerical simulation of transmembrane potential distribution. Additionally, gwiz SEAP are relatively large plasmids, and they may experience strong stretching in the converging direction of the micronozzle,^{15,16} leading to easier binding and delivery through the cell membrane.

Comparison of MSE with Bulk Electroporation and Nucleofection. Results of gWiz SEAP transfection of mouse ES cells by micronozzle array enhanced MSE, bulk electroporation using Bio-Rad Gene Pulser, and nucleofection are compared in Figure 4. Although the transfection result of MSE was still not as good as that of nucleofection using unknown cell-specific reagents, the amount of SEAP expression mediated by the MSE method was higher than that in bulk electroporation by Bio-Rad Gene Pulser X-Cell system using the same electroporation buffer. The main reason is that the MSE method is able to preconcentrate the genes near the cell surface and to focus the electric field strength around the micropores for better gene transport during electroporation.

The averaged electric field strength applied in MSE was 150 V/cm, but it could generate a higher local electric field in the microchannel or micronozzle than that in bulk electroporation, i.e. ~ 500 V/cm. Also, the affected area of cell membrane in MSE is much smaller than that in bulk electroporation as shown in Figure 6b. Therefore, mouse ES cells experienced an average survival rate of $\sim 75\%$ in MSE with an initial cell number of $1 \times$

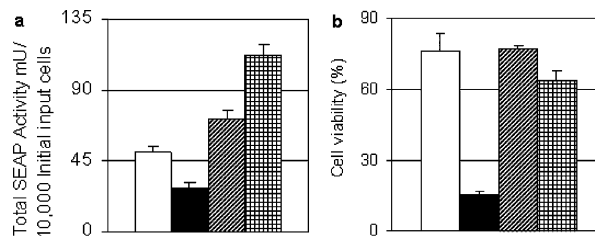


Figure 4. Comparison of mouse ES cell transfection by micronozzle array enhanced MSE, bulk electroporation by Bio-Rad Gene Pulser, and nucleofection. (a) Transfection efficiency and (b) cell viability 24 h after electroporation. From left to right, bulk electroporation with initial input cell number of 1×10^6 (□) and 1×10^5 (■); micronozzle enhanced MSE with initial input cell number of 1×10^4 (▨); and nucleofection with initial input cell number of 1×10^6 (▩).

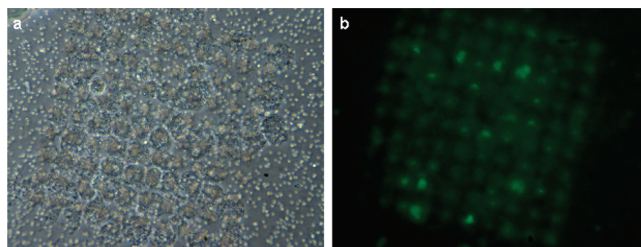


Figure 5. GFP transfection of mouse ES cell by micronozzle enhanced MSE. A hundred cells were trapped on a 10×10 micronozzle array, and (a) phase contrast and (b) fluorescent images were taken 24 h after electroporation.

10^4 , similar to that in bulk electroporation with 1×10^6 initial cells and much higher than that in bulk electroporation with 1×10^5 initial cells.

MSE can provide high transgene efficiency and cell viability because the area of cell membrane with the highest transmembrane potential is the same location that negatively charged DNA molecules could permeate into the cells during electroporation.¹⁷ On the other hand, a much larger area of cell surface would experience very high electric field strength in the bulk electroporation, even though DNA molecules cannot transport across most of the affected cell surface. This difference will be further elaborated on later by numerical simulation of transmembrane potential distribution on the cell surface.

Since only a small area of cell membrane is affected during MSE and each cell can experience a similar electric field with a micronozzle array, a very small number of cells could be uniformly transfected by this method. As an example, a hundred mouse ES cells trapped on a 10×10 micronozzle array were transfected by pmaxGFP. Mouse ES cells were analyzed 24 h after electroporation by phase contrast and fluorescence microscopy using a GFP filter. One result is shown in Figure 5. Almost all the cells were transfected and remained alive, a performance not achievable by other electroporation methods. This indicates the potential of micronozzle array enhanced MSE for hard-to-harvest cells.

Simulation of Transmembrane Potential Distribution. The electroporation mediated gene transfection process includes two major steps: (1) cell membrane breakdown and reseal and (2) genes bounding to the cell membrane during the electroporation and entering cell plasma by endocytosis. If the transmembrane

(15) Wang, S.; Hu, X.; Lee, L. J. *Lab Chip* **2008**, 573–581.

(16) Hu, X.; Wang, S.; Lee, L. J. *Phys. Rev. E* **2009**, 79, 041911.

(17) Golzio, M.; Teissié, J.; Rols, M.-P. *Proc. Natl. Acad. Sci. U.S.A.* **2002**, 99, 1292–1297.

potential is larger than the critical transmembrane potential under an imposed external electric field, the cell membrane becomes permeable. Since the distribution of transmembrane potential is extremely critical to the cell transfection, we calculate this distribution in both a bulk and micropore based membrane sandwich electroporation using numerical simulation.

In this study, we simplify the cell with a three-layer (or single-shell) model and solve the equations in the internal cytoplasm, the external medium, and the cell membrane, respectively. The Laplace equation of the three-layer model¹⁸ is used to calculate the distribution of the electric field and transmembrane potential (the potential difference across the cell membrane) of a single cell in bulk electroporation and MSE:

$$\nabla \cdot (\sigma_i \nabla \varphi_i) = 0 \quad (1)$$

$$\nabla \cdot (\sigma_e \nabla \varphi_e) = 0 \quad (2)$$

$$\nabla \cdot (\sigma_m \nabla \varphi_m) = 0 \quad (3)$$

where ϕ is the electric potential, σ is the electric conductivity, “i” is the internal cytoplasm, “e” is the external medium, and “m” is the cell membrane.

Correspondingly, there are two boundary conditions (BCs) for two interfaces, i.e., the external interface between the external medium and the cell membrane and the inner interface between the cytoplasm and the cell membrane.

BCs on external interface:

$$\sigma_e \frac{\partial \varphi_e}{\partial n} = \sigma_m \frac{\partial \varphi_m}{\partial n} \quad (4)$$

$$\varphi_e = \varphi_m \quad (5)$$

BCs on internal interface:

$$\sigma_i \frac{\partial \varphi_i}{\partial n} = \sigma_m \frac{\partial \varphi_m}{\partial n} \quad (6)$$

$$\varphi_i = \varphi_m \quad (7)$$

In our experiments, a low-conductive PET membrane was used as solid walls, and thus, the electric field across the PET membrane can be neglected. Therefore, all solid walls are treated as insulators. Different potentials are imposed at the inlet and outlet in order to create a voltage drop. Once the electric potentials are calculated, the electric field \mathbf{E} could be known at different layers:

$$\mathbf{E} = -\nabla \varphi \quad (8)$$

The transmembrane potential is obtained as

$$\Delta V_m = \varphi_m(S_{\text{ext}}) - \varphi_m(S_{\text{int}}) \quad (9)$$

where S is the surface of cell membrane, “ext” is the external, and “int” is the internal.

Table 2. Parameters of the Three-Layer Model²⁰

symbol	value	definition
d	5 nm	cell membrane thickness
σ_e	0.2 S/m	electric conductivity of external medium
σ_i	0.2 S/m	electric conductivity of cytoplasm
σ_m	5×10^{-7} S/m	electric conductivity of cell membrane

Compared with the two-layer model simulation,¹⁹ the three-layer model simulation is more complicated and the very dense mesh needs to be generated near the cell membrane. However, it can be easily applied to calculate the transmembrane potential around electroporated cells with nanopores formed on the cell membrane. Since the breakdown of cell membrane occurs very quickly (in the order of microseconds) after turning on the electric field, we assume that the external voltage drop between two electrodes is constant during such a short period of time. The calculated transmembrane potential is an initial value because it reflects the potential difference across the cell membrane before its breakdown.

Since the three-dimensional (3-D) simulation is complicated and time-consuming, a two-dimensional (2-D) simulation with the three-layer model is carried out using commercial FEM software, COMSOL (Mathworks, Natick, MA). Parameters used in the simulation are given in Table. 2.

For a single 2-D circular cell in bulk electroporation, we have verified that the calculated transmembrane potential by numerical simulation agrees well with the analytical solution, which is given by the following equation:¹⁸

$$\Delta V_m = fER\cos(\theta) \quad (10)$$

where E is the external electric field strength (V/cm), R is the radius of the cell (μm), θ is the facing angle between E_{ext} and the point on the cell membrane, and f is the shape factor; $f = 2$ for a 2-D circular cell.

Mouse ES cells with an average diameter of 10 μm were used in the experiments. In bulk electroporation, cells are suspended in buffer solution and, thus, are simplified as a circular shape with the diameter of 10 μm in 2-D simulation. In MSE, the cells are placed on a flat surface with slight deformation caused by the gravity effect of the cell itself and the compression effect from the top membrane when the membrane–membrane distance is less than 5 μm . As observed from an inverted microscope, the average diameter of the cells is 15 μm in the X–Y cross-section area, and thus, we simplify the cell shape as an ellipse with the major axis of 15 μm and the minor axis of 4.5 μm in MSE.

For simplicity, we assume that microchannels on the top membrane are uniformly distributed in the simulation. The thickness of the top membrane is 10 μm , and the size of a microchannel is $\sim 1 \mu\text{m}$. According to the pore density of 1.6×10^6 pores/ cm^2 given in the manufacturer’s instruction, the center-to-center distance between two microchannels is 7.7 μm . For the cell binding membrane, the thickness is 12 μm and the center-to-center distance between two micronozzles or microchannels

(18) Stewart, D. A.; Gowrishankar, T. R.; Smith, K. C.; Weaver, J. C. *IEEE Trans. Biomed. Eng.* **2005**, 52, 1643–1653.

(19) Zudans, I.; Agarwal, A.; Orwar, O.; Weber, S. *G Biophys. J.* **2007**, 92, 3696–3705.

(20) Kotnik, T.; Bobanović, F.; Miklavčič, B. *Bioelectrochem. Bioenerg.* **1997**, 43, 285–291.

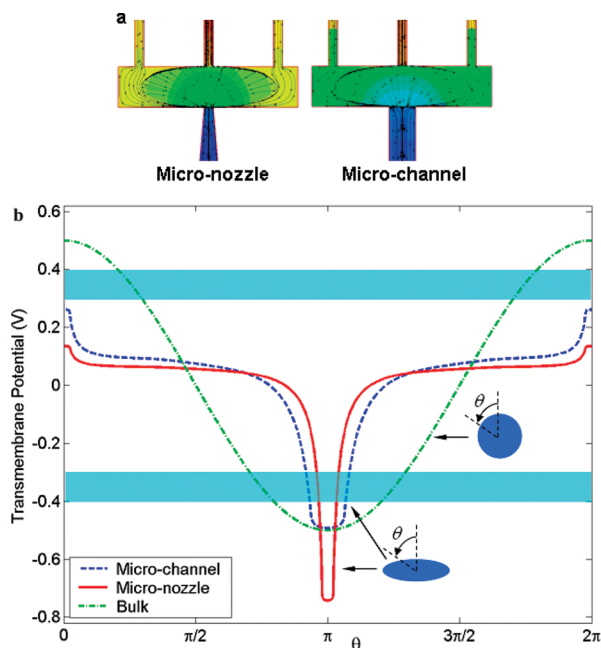


Figure 6. Simulation comparison between MSE and bulk electroporation: (a) electric potential distribution and electric field lines across/around a single cell near a micronozzle (left) and microchannel (right), and (b) calculated transmembrane potential distribution. θ is the facing angle around the cell surface. In addition, two bands are added to indicate the areas of critical transmembrane potential (with an absolute value around 0.3–0.4 V).

is 20 μm . The procedure of 2-D finite element simulation for the electroporation of a circular or an oval cell starts from the mesh generation, followed with the calculation of potential and electric field. Finally, the transmembrane potential was calculated using eq 9. The simulation results are given in Figure 6.

Figure 6a shows that the electric field is concentrated around the micropore, and more electric field lines are forced to penetrate through the cell at the small-end of the micronozzle. Correspondingly, the transmembrane potential at the small-end of the micronozzle is higher than that of the straight channel as shown in Figure 6b. This explains why our micronozzle MSE can provide better delivery efficiency than the microchannel MSE, as shown in Figure 3.

Micronozzle and microchannel enhanced MSE is also compared with bulk electroporation. As shown in Figure 6b, a much broader transmembrane potential distribution is observed in bulk electroporation. In order to reach the same maximum transmembrane potential observed in the microchannel enhanced MSE, a much higher electric voltage, 500 V/cm instead of 150 V/cm, needs to be used in bulk electroporation. Although a larger area of cell surface experiences high electric field strength in bulk electroporation, it may not be helpful because the transgene efficiency does not depend on the total area of cell membrane with openings but on the effective area facing the cathode.²⁰ In fact, a larger affected cell surface often leads to a higher cell damage rate. This is why the MSE method is able to provide better cell viability in electroporation.

To verify the applicability of the calculated transmembrane potential, we used propidium iodide (PI; Molecular Probe, Catalog

No. P3566), a red-fluorescent dye excluded from viable cells with an intact cell membrane, to demonstrate nanopore formation on the cell surface when the imposed transmembrane potential is higher than a critical value. This positively charged dye can easily diffuse into the cell, and the cell will turn bright if nanopores are formed on the cell membrane. For bulk electroporation, 1×10^5 cells were mixed with high glucose DMEM containing 100 μM PI, and the sample solution was loaded in a reservoir. For MSE, 100 cells were trapped on an 10×10 array, and high glucose DMEM with and without 100 μM PI were loaded in the bottom and top channel of the MSE device, respectively. When an exponentially decay pulse to the system is applied, the critical electric field strength observed was ~ 300 V/cm for bulk electroporation, and ~ 75 V/cm for MSE. This indicates that the focused electric field enhances cell permeation at a low electric voltage in the MSE method. The calculated critical transmembrane potential is ~ 0.3 V for bulk electroporation and ~ 0.375 V for MSE, similar to values reported in the literature. If we assume that the critical transmembrane potential for PI dye diffusion into mES cells is 0.3–0.4 V, the calculated highest transmembrane potential on the cell surface shown in Figure 6 exceeds this critical value for bulk electroporation and both MSE methods. This agrees fairly well with the observed PI dye results. More sophisticated modeling and computation is needed to simulate the complete gene transfection process.

CONCLUSION

In this study, we demonstrated the use of femtosecond laser fabricated micronozzle arrays on a gelatin-coated PET membrane for membrane sandwich electroporation (MSE). Using micronozzle array based sandwich electroporation, we observed high and uniform gene transfection and good cell viability of mouse ES cells compared to the bulk electroporation. Numerical calculation of transmembrane potential and the PI dye diffusion experiments qualitatively explain the observed differences between MSE and bulk electroporation.

The strategy of ex vivo stem cell based therapy includes genetically modifying stem cells in vitro and then implanting them in vivo under pharmaceutical standards. Successful preclinical trials of transfecting stem cells using in vitro electroporation have been demonstrated for bone repair²¹ and dentin formation.²² Since patient cells are often very limited, the ability to treat a small number of cells (i.e., hundreds or thousands) using our MSE method, instead of millions of cells required in a single bulk electroporation process, offers great potential for hard-to-harvest primary cells in patient-specific ex vivo gene therapy because many electroporation tests maybe needed to provide necessary in vitro pharmaceutical kinetic data for a specific gene delivery.

ACKNOWLEDGMENT

This work was supported by the National Science Foundation under Grant No. EEC-0425626.

SUPPORTING INFORMATION AVAILABLE

Additional information as noted in text. This material is available free of charge via the Internet at <http://pubs.acs.org>.

Received for review September 10, 2009. Accepted November 2, 2009.

AC902041H

(21) Aslan, H.; Zilberman, Y.; Arbeli, V.; et al. *Tissue Eng.* **2006**, *12*, 877–889.

(22) Nakashima, M.; Iohara, K.; Ishikawa, M.; et al. *Hum. Gene Ther.* **2004**, *15*, 1045–1053.